Available online at www.sciencedirect.com

Chemical Engineering Research and Design

journal homepage: www.elsevier.com/locate/cherd

Performance study of novel PES membrane using electrospray deposition method for organic contaminants separation

Buthayna Al-Ghafri[a], *Htet Htet Kyaw*[a], *Mohammed Al-Abri*[a,b,*], *Woei-Jye Lau*[c]

[a] *Nanotechnology Research Centre, Sultan Qaboos University, PO Box 17, PC 123, SQU, Al-Khoudh, Oman*
[b] *Department of Petroleum and Chemical Engineering, College of Engineering, Sultan Qaboos University, PO Box 33, PC 123, SQU, Al-Khoudh, Oman*
[c] *Advanced Membrane Technology Research Centre (AMTEC), Universiti Teknologi Malaysia, 81310 Skudai, Johor, Malaysia*

ARTICLE INFO

Article history:
Received 25 May 2022
Received in revised form 8 July 2022
Accepted 20 July 2022
Available online 22 July 2022

Keywords:
Polyethersulfone Membrane
Electrospraying
Electrospinner
Bovine serum albumin
Humic acid
Wastewater treatment

ABSTRACT

The aim of this study is to design and fabricate a new kind of membrane that could be used effectively in wastewater treatment. In this study, a novel type of electrosprayed thin membrane was synthesized via electrospray deposition technique and its properties were compared with electrospun membrane in terms of structure and separation efficiency. The electrosprayed thin membrane was developed using dope solution composed of 20 wt. % polyethersulfone (PES) and 80 wt. % n-methyle-2-pyrrolidone/dimethylformamide mixture. The electrosprayed PES membrane exhibited water flux of up to 100 $Lm^{-2}h^{-1}$ at 2 bar with porosity of 76 % which is very similar to the electrospun membranes. The electrosprayed PES membrane also showed an excellent tensile strength up to 4.5 MPa and demonstrated about 81 % and 63 % rejection rate against humic acid (HA) and bovine serum albumin (BSA), respectively when tested at 2 bar. The fouling of the membrane was further studied using FTIR, TGA and XPS analysis and the results confirmed that the membrane did not suffer from substantial fouling. Moreover, a high flux recovery was recorded, indicating low fouling tendency of the membrane. Overall, the findings showed that the electrosprayed thin PES membrane performed better than the electrospun PES membrane for wastewater treatment.

1. Introduction

Globally, there is an increasing demand for clean water for drinking and agricultural uses. However, the vast majority of the world's water is seawater and is not potable. The small remaining amount available is often polluted. As a result, it is essential to find technologies that can effectively treat and recycle wastewater. Many different separation technologies have been implemented but each has its own limitations. Currently, membrane technology is being used worldwide and is showing a good deal of promise. This technology is mainly dependent on the size of the pores and the surface charge of the membrane, which act as a physical barrier, and on the molecular size of the constituents present in wastewater. Membranes with different pore size range can be classified into porous membranes such as microfiltration (MF) and ultrafiltration (UF) or dense membranes such as nanofiltration (NF) and reverse osmosis (RO) (Baker and Staff, 2000; Kassa et al., 2020; Khin et al., 2012).

* Corresponding author at: Nanotechnology Research Centre, Sultan Qaboos University, PO Box 17, PC 123, SQU, Al-Khoudh, Oman. E-mail address: alabri@squ.edu.om (M. Al-Abri).
https://doi.org/10.1016/j.cherd.2022.07.028

MF membrane is used for pre-treatment applications in the removal of submicron materials suspended in water, including bacteria and algae sediments with a molecular size in the range of 0.01–1 μm. By contrast, UF membranes with pore size of 10–100 nm are used for the removal of dissolved organic matters and pathogens like viruses and proteins (Baker and Staff, 2000; Chabalala et al., 2021; Vatanpour et al., 2020). However, several studies have reported that proteins and organic contaminants may cause severe damage to these membranes due to their accumulation/deposition on the membrane surface and/or within their pores (Bidlack and Tappel, 1973; Khulbe et al., 2007; Mo et al., 2008). Typically, bovine serum albumin (BSA) with molecular weight (MW) of 66.5 kDa is a model foulant used to determine UF membrane performance. Considerable attention has been paid to BSA in biomedical applications (Buddanavar and Nandibewoor, 2017) and also in separation process research using membranes (Zhao et al., 2016; Zhu et al., 2015). Aside from BSA, researchers have also looked at the presence of organic contaminants like humic substances in water sources as they can easily react with disinfectant products like chlorine to form harmful disinfection by-products (DBPs) such as haloacetic acids (HAAs) and trihalomethanes (THMs) (Ma et al., 2014; Rojas and Horcajada, 2020; Wang et al., 2019).

Another key factor is the choice of membrane. Polymeric membranes have been shown to be outstandingly effective in wastewater treatment, with polyethersulfone (PES) being one of the most frequently used polymers for this application, owing to its high selectivity, cost effectiveness, high rejection rate and excellent mechanical strength (He et al., 2017; Lalia et al., 2013; Moradi et al., 2020). The attractiveness of these properties can be further improved by enhancing the membrane porosity, hydrophilicity and charge density. The major drawback of conventional UF membranes however is surface fouling. This results in a reduction in net water flux, higher pressure drop and shorter membrane lifespan.

Electrospun nanofiber membranes outclass other membrane types because of their large surface area and high porosity. They are also simple to set up. However, in spite of these special features, nanofibrous membranes are not very efficient for the removal of macromolecular substances and are therefore mainly used in pre-treatment (Gopal et al., 2006; Homaeigohar et al., 2010; Missau et al., 2018). Another important factor to consider is the mechanical strength of these membranes. Generally, electrospun nanofibers provide good mechanical stability as has been reported by Al-Ghafri et al. (2018) and Al-Husaini et al. (2019a, 2019b), but, their hydrophobic character may result in a greater tendency to fouling.

This study sought to overcome the drawbacks of both UF membranes and electrospun membranes by designing and fabricating a highly porous electrosprayed membrane with pore size greater than 100 nm and high solute retention. Moreover, the membrane with interconnected pore structure is expected to operate at low hydrostatic pressure and can achieve better filtration performance than typical asymmetric flat sheet membranes.

There are other reasons why electrosprayed membranes are favoured over electrospun and conventional flat membranes. The electrospraying process is an electrohydrodynamic process, where a jet breaks into drops (< 1 μm) when a high voltage/potential is applied between the collector and the nozzle in the electrosprayer. The working principle of this electrospraying process is similar to that in electrospinning (Bhardwaj and Kundu, 2010; Deitzel et al., 2001; Sweet et al., 2014; Tański et al., 2017); however, the viscosity of the polymer makes the electrospraying process more effective. At a lower concentration, the polymer can be sprayed with a high-voltage electric field to produce particles instead of fibers; these have excellent self-dispersion attributable to Coulombic repulsion (Selatile et al., 2018). The key advantage of using electrospraying over the casting method is that the thickness of the membrane can be controlled, so that a thinner and more uniform membrane can be achieved. Electrospraying membranes also have the potential to overcome the limitations of conventional casting membranes because they use lower amount of dope solution, and operate at lower pressure as a result of their lower hydraulic resistance (Bonyadi and Chung, 2007; Selatile et al., 2018; Tsai et al., 2000; Wang et al., 2022; Yang et al., 2009). They also have more efficient liquid flux, as well as better porosity, greater mechanical strength and longer durability (Idris et al., 2002; Shaulsky et al., 2017).

Several other factors are central to the formation of the particles and thus the uniformity of the membrane. The selection of the solvent used in the dope solution has a critical role in the particle size, and the solvent's evaporation rate has also been proved to affect the quality of the particle formation (Takeshi et al., 2013). Other important parameters of electrospraying process are flow rate, humidity, voltage and distance between collector and nozzle. Furthermore, the uniformity of the membrane is mainly dependent on the particle diameter, as the smaller the diameter of the particle, the higher the quality of the membrane. The aim of this study is to design and fabricate a new kind of electrosprayed thin membrane that could be used effectively in wastewater treatment. The developed membranes will be evaluated with respect to water permeability and solute rejection while its intrinsic properties will be characterized. using a series of instruments including tensile testing machine, optical contact angle (CA) goniometer, scanning electron microscope (SEM), Fourier transform Infrared (FTIR) spectroscope, thermogravimetric analyzer (TGA) and X-ray photoelectron (XPS) spectroscope.

2. Methodology

2.1. *Materials*

All materials used in this study were purchased from a number of reputable sources. PES (granular size: 3 mm) was purchased from Goodfellow Limited in Cambridge, UK (PE29 6WR); dimethyl formamide (DMF) from Sigma-Aldrich; n-methyl-pyrrolidinone (NMP) from Fluka Analytical (Germany); bovine serum albumin (BSA, Fraction V powder 96 %, MW: 66.5 kDa) and humic acid (HA) from Fisher Scientific. The DI water used for all experiments was produced by the Milli-Q system (O-Purite).

2.2. *Electrosprayed thin membrane*

There were several stages in the fabrication of the electrosprayed thin membrane. First, the PES pellets were dried overnight in an oven at 70 °C to remove moisture. After that, it was gradually added to a preweighted solvent mixture. The dope solution was made by dissolving 20 wt. % of PES in a mixture of DMF/NMP solvent with three different DMF:NMP volume ratios (i.e., 0:1, 1:4 and 2:3). The respective solution

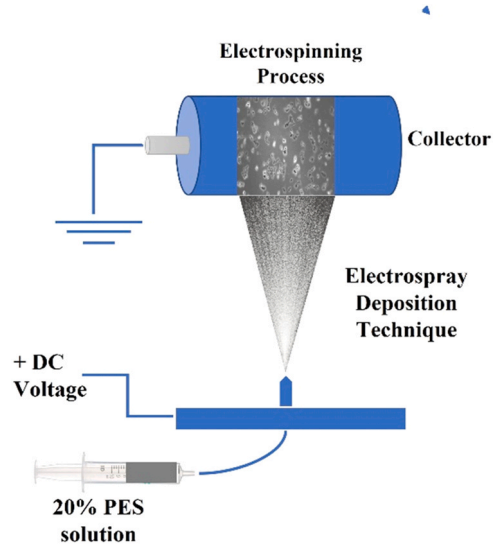

Fig. 1 – Fabrication of novel PES membrane based on electrospray deposition technique using multi-nozzle nanospinner.

Table 1 – Electrospinner parameter for electrospun membrane and electrosprayed membrane.

Membrane type	Electrospun membrane	Electrosprayed membrane
Flow rate (mL/hr)	1:00	1:20
Voltage (kV)	23.5	20.4
Spinneret distance (mm)	130	130
Humidity %	60	60
Speed (rpm)	220	220

was stirred continuously for 48 h at 80 °C in order to homogenize the mixture. The prepared dope solution was then electrosprayed onto an aluminium foil using a multi-nozzle nanospinner (NS24) for 4 h as shown in Fig. 1 with the synthesis conditions as shown in Table 1. The resultant membrane was allowed to dry inside the chamber of electrospinner for 24 h before it was taken out.

The membrane was dried inside the electrospinner instrument for 24 h before it was taken out. Separately, an electrospun PES membrane was also prepared using a dope composed of 26 % PES and 74 % DMF/NMP (7:3) mixed solvent. The electrospinning conditions for PES nanofiber mat are shown in Table 1. The PES solution was electrospun onto an aluminium foil using a multi-nozzle nanospinner (NS24). The membrane was only taken out from the chamber 24 h after completing the electrospinning process.

2.3. Membrane characteristics

2.3.1. Membrane morphology

A scanning electron microscope (JEOL, JSM-7600 F FESEM), operating at 20 kV, was used to analyse the morphology of the fabricated membrane. Before the SEM image analysis was conducted, the membrane sample had to be prepared. First, a cross-section of the fabricated membrane was obtained by freezing it with liquid nitrogen to avoid the collapse of the porous structure; this was then fractured. Afterwards, the prepared sample was coated with platinum to avoid the effects of electrons charging. After these preparations, the SEM image analysis was conducted.

The mechanical properties of the prepared membranes were measured using an instron tensile machine (Tinius Olsen-H5KT). Membrane pieces measuring 2 cm × 3 cm was used for the tensile test, with the following instrument parameters, i.e., 180-mm gauge length, 110-μm specimen thickness and 20-mm width (at the centre). The true stress-true strain curve was plotted and was used to calculate the tensile properties such as ultimate strength and elongation at the break point.

Water contact angle (WCA) of membrane was measured using an Optical Tensiometer instrument (Biolin) to evaluate the surface hydrophobicity of the membranes. A sessile drop was set to 5 μL and samples of 2 cm × 3 cm size were put on a glass slide. Three measurements were taken for each membrane sample to yield an average value. The viscosity measurement was conducted using Rheometer (Bholin Gemini 150, Malvern) to study the effect of PES weight on the viscosity of PES polymeric solution. The results are provided in Fig. S1.

2.3.2. Porosity

The overall porosity of the fabricated membrane (ε, %) was measured by applying the dry-wet weight equation as follows,

$$\varepsilon = \left(\frac{\frac{(W_w - W_d)}{\rho_{H_2O}}}{\frac{(W_w - W_d)}{\rho_{H_2O}} + \frac{W_d}{\rho_{PES}}} \right) \times 100 \quad (1)$$

where W_w and W_d are the weight (g) of the wet and the dry membrane, respectively; ρ_{H_2O} is the pure water density (0.998 g/cm^3) and ρ_{PES} is the PES density (1.37 g/cm^3). The thickness of the membranes was measured using a digital micrometer (Mitutoyo) and it was found to be 110 μm (Eq. (2)).

To estimate the pore size (r_m), the Hagen-Poiseuille equation was used (Hernández et al., 1996; Wang et al., 2017).

$$r_m = \sqrt{\frac{8\mu\Delta x J}{\varepsilon_v \Delta P}} \quad (2)$$

where Δx is the thickness of membrane, μ is viscosity of water (8.9 ×10^{-4} Pa s) at 25°C, ε_v is the obtained porosity, J is the flux (m^{3}s^{-1}) per area (A) and ΔP is the applied pressure (Pa).

2.4. Filtration tests

Filtration tests were carried out using a dead-end cell (01730, Amicon, Millipore MA) at room temperature. The aim was to determine the pure water flux, the BSA and HA flux, and the solute retention. Before testing, the membranes were cut into a circular shape, so that the effective surface area of the membrane was 28.7 cm^2. To prepare for the water flux (J_0) testing, the membrane was compacted at 5 bar and was kept in deionized water for one day to ensure that all the pores were filled with water. The membrane sample was then placed within the dead-end cell, with the active skin layer facing upwards.

The average water flux, J (L.m^{-2}.h^{-1}) was determined by measuring the permeate every 15 min for the first hour, and then every 30 min for the next 2 h using Eq. (3).

$$J = \frac{V}{A\Delta t} \quad (3)$$

where V (L) is the volume of the permeate at the period of time Δt (h) and A (m^2) is the effective area of the membrane. The dead-end cell identified above was also used in the BSA and HA rejection testing. 2 bar of nitrogen gas was used to test the electrosprayed thin membrane during the whole process.

2.4.1. *Rejection*

BSA was used to evaluate the filtration performance of the fabricated membranes. A BSA calibration curve was constructed by measuring the optical absorbance of BSA (100–500 ppm) solutions, which were prepared in DI water. The BSA concentration was used directly for the measurements to ensure that the protein did not denature (Miron et al., 2019). The concentration of the filtrated BSA was measured using an absorbance peak at a wavelength (λ) of 280 nm of permeated protein using UV–vis light (Ocean Optic, USB4000).

The rejection rate (%) of BSA was calculated using Eq. (4).

$$\text{Rejection} = \left(1 - \frac{C_P}{C_F}\right)\text{x}100 \quad (4)$$

where C_p is the BSA concentration in the permeate solution and C_F is the BSA concentration in the feed solution.

For the performance test investigation, HA was used, with the same measurement process as was used for BSA. To prepare for the investigation, HA was dissolved in basic media in a pH of 9, which was adjusted by NaOH. 50 ppm of HA solution was prepared by dissolving 50 mg of HA in 1 L of ultrapure water. The feed solution was then poured into a dead-end cell before the filtration experiment process was started. The membranes were cleaned and rinsed thoroughly with DI water, and then soaked in DI water for a further 1–2 h before the water flux recovery measurements were obtained.

2.5. *Membrane stability*

Several fouling tests were conducted to assess the electrosprayed PES membrane. Thermogravimetric analysis (TGA, PerkinElmer Pyris STA 6000, Germany) was used to evaluate the thermal property of the electrosprayed PES membrane before and after the rejection tests. TGA tests were conducted from 30 °C to 900 °C using 19–21 mg of the prepared membrane at a constant rate of 10 °C/min^{-1} under nitrogen atmosphere.

A PerkinElmer Frontier FT-IR spectroscope from USA was used to study the surface group of the electrospray PES membrane. The spectra were recorded in the range of 500–4000 cm^{-1} and scanned 32 times with a resolution of 4 cm^{-1}.

The study sought to confirm the fouling results by carrying out XPS measurements using photoelectron spectroscopy (Scienta Omicron, Germany) equipped with Al K-alpha X-ray source as excitation. For survey spectra, pass energy of 50 eV was used and 20 eV was employed for high resolution spectra. In order to neutralize the surface charging, a flux of electron beam was applied onto the sample surface during measurement. XPS spectra were analyzed using Casa XPS (Casa XPS software Ltd., UK) with Gaussian Lorentzian (30,70) function without background subtraction. Intrinsic carbon peak at 284.6 eV was utilized as reference binding energy and calibrated accordingly.

Moreover, pure water recovery (PWR, %) was recorded to study the membrane fouling due to HA and BSA molecules accumulation. The membranes were rinsed with DI water after the rejection tests and the pure water flux recovery was measured using Eq. (5).

$$\text{PWR} = \left(\frac{J_{W2}}{J_{W1}}\right)\text{x}100 \quad (5)$$

where J_{w1} is the pure water flux of the membrane before rejection tests and J_{w2} is the pure water flux after rejection tests. The washing process lasted 30 min under same condition as rejection test.

3. Results and discussion

3.1. *Membrane morphology*

Different percentages of a PES polymeric solution were investigated using viscosity measurement (Fig. S1) and SEM micrograph (Fig. 2 and S2). The viscosity was measured in the range of 15–30 wt. % and the SEM micrographs of the formed membranes at lower than 20 % PES and higher than 26 % PES are shown in Fig. S2. Part of the results is based on our previous research work published elsewhere (Al-Ghafri et al., 2018). When the PES concentration was higher than 21 wt. %, fibers started to form, initially with some particulates. However, when the critical entanglement concentration was reached, uniform fibers were formed. When the polymer concentration was too high (viscosity > 6000 cP), beaded fibers were produced. However, at a viscosity lower than 705 cP and this solution could not be electrospun via a nanospinner instrument and a phase inversion method had to be used instead (Al-Hinai et al., 2017). It was found that at 20 wt. % the viscosity of PES solution was around 700 cP, the

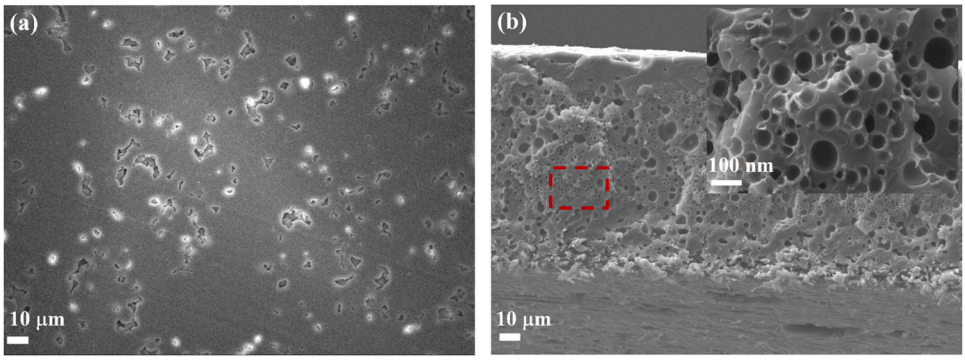

Fig. 2 – PES membrane morphology with 20 % PES concentration using a nanospinner instrument; (a) top view and (b) cross section view.

Table 2 – Porosity and pore radius of fabricated membranes.

Membrane	ε (%)	r_m (μm)
Electrospray PES	76.32	0.103

polymeric solution could be then electrosprayed using an electrospinner, forming a new type of membrane.

The morphology of this new membrane was further studied using SEM images, with the findings are shown in Fig. 2. It was found that when PES concentration was at 20 wt. %, droplets were formed instead of fibers. The top view SEM micrograph of the electrosprayed PES membrane (Fig. 2a) showed a porous surface and the cross-section (Fig. 2b) clearly showed that the membrane has an asymmetrical structure composed of a thin, porous skin structure with a thickness of 110 μm. The magnified SEM micrograph in Fig. 2b (inset) shows that the interconnected pores are in micro-scale range and the calculated data (pore size and porosity) are presented in Table 2. A mixture of two aprotic solvents (20 wt. % DMF in NMP) was used to prepare a PES polymeric solution that would form the electrosprayed thin PES membrane. A higher amount of NMP was used in the mixed solvent, because NMP could results in a more homogenous and less viscous solution. It was found that dissolving PES polymer in certain solvents such as DMF could turn the solution to a gel-like mixture over time (Al-Hinai et al., 2017). Since 20 wt. % PES solution was able to produce a new type of membrane, it was selected for further evaluation in this study.

3.2. *Mechanical properties*

The mechanical strength of the electrosprayed PES membrane fabricated in the study was investigated by analysing its mechanical properties. First, it was assessed using a true stress-true strain curve, as shown in Fig. S3. The tensile strength and elongation-at-break were then calculated and the results were compared with an electrospun PES membrane as shown in Fig. 3. The tensile strength of the electrosprayed PES membrane was 4.48 MPa which was significantly greater than that of the electrospun PES membrane (2.90 MPa) (Al-Ghafri et al., 2018; Al-Husaini et al., 2019a). However, the elongation-at-break point of the electrospun membrane indicated that this membrane was more elastic by 28 %. It is generally known that the electrospun membrane tends to offer a progressive dealignment of its nanofiber which gives the membrane a greater elongation capability before rupture. However, the presence of interconnected pore structure in the electrosprayed membrane is believed to offer greater physical properties in terms of compaction compared to the electrospun nanofiber membrane during filtration process.

3.3. *Pure water flux and hydrophilicity*

Fig. 4 shows that the WCA of the electrosprayed thin membrane was around 93° which was lower compared to the electrospun membrane of 126°. This indicated that the electrosprayed membrane was less hydrophobic than that of electrospun membrane. With respect to flux, the recorded pure water flux for the electrosprayed PES membrane was 101.6 L $h^{-1}m^{-2}$ at 2 bar which was similar to the electrospun

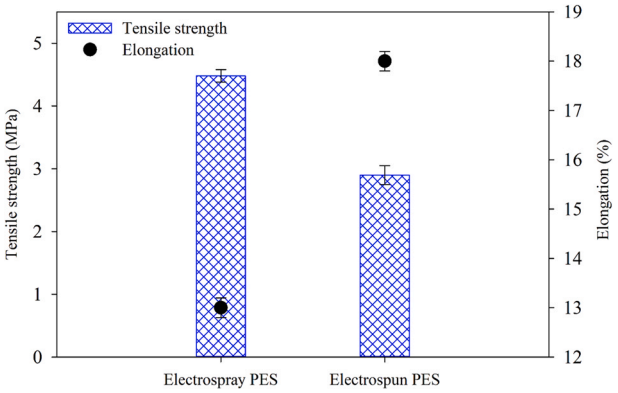

Fig. 3 – Tensile strength and elongation-at-break of electrosprayed PES membrane and electrospun membrane.

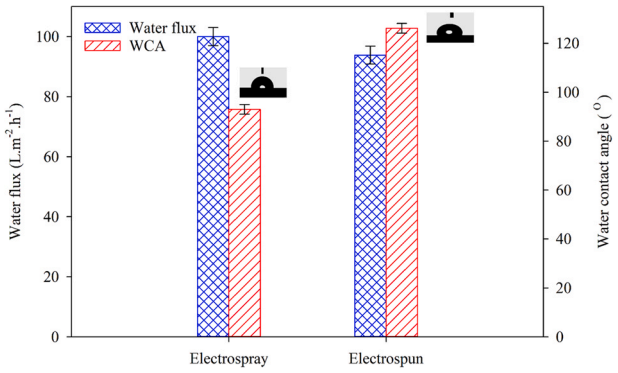

Fig. 4 – Pure water flux and water contact angle of electrosprayed and electrospun membrane.

membrane but higher than that reported for the UF membrane at 10 bar pressure (Al-Hinai et al., 2017). This is due to the interconnected pore structure in the electrosprayed PES membrane (SEM image in Fig. 2b), which creates pathways for water to flow freely through the membrane. It is also attributable to the high porosity and larger pore size distribution (see Table 2).

3.4. *Rejection and filtration flux of BSA protein and HA*

A selectivity test was performed to study the effectiveness of the electrosprayed membrane in rejecting 50 ppm HA and 150 ppm BSA and the results are presented in Fig. 5. The electrosprayed membrane recorded a removal rate of against 62.4 % BSA. This result can be compared with those from previous research using electrospun membrane. For example, when an electrospun PSF membrane was used, around 10 % of BSA was removed (Uzal et al., 2017). It was not possible to compare results for nanofibers membranes, since there have been almost no serious trials using nanofiber for BSA rejection. This is because of the large pore size of electrospun membranes that makes them inefficient to separate these kinds of molecules from water (Bae et al., 2016).

The membrane fabricated for this study also achieved a better rejection rate for HA than other types of membranes. When tested using 50 ppm HA solution, the rejection of membrane was found at 80.6 % which was remarkably better than the electrospun membrane reported in another study (Al-Ghafri et al., 2019). In both tests, the rejection was mainly due to the hindrance effect of the membrane since a dead-end cell was used in this work and the feed solution was being stirred and no protein or acid substances were

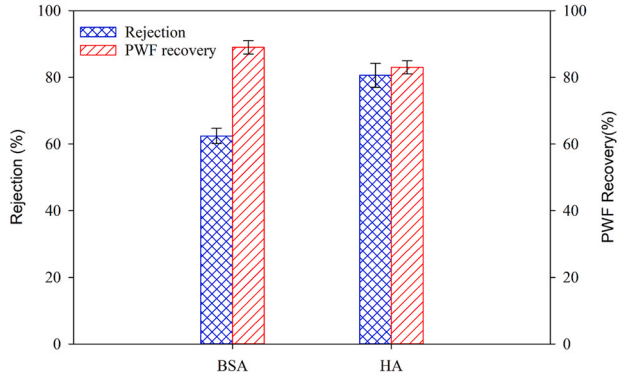

Fig. 5 – BSA [150 ppm] protein and HA [50 ppm] molecule rejection and pure water flux recovery of electrosprayed membrane at 2 bar.

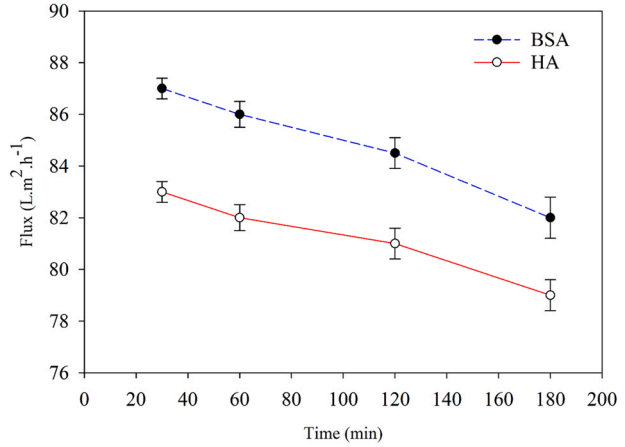

Fig. 6 – Water flux of electrosprayed membrane in filtrating BSA [150 ppm] protein and HA [50 ppm] at 2 bar for 3 h.

expected to accumulate on the membrane layer. Moreover, a high flux recovery was recorded after the rejection tests as shown in Fig. 5. This indicated lower fouling tendency of the membrane. BSA and HA fluxes were lower than that of pure water flux as clearly shown in Fig. 6 mainly because of presence of HA and BSA in the feed solution. By comparing the separation performance of membrane against two types of solutes, the electrosprayed membrane showed a higher HA rejection rate (81 %) compared to the BSA (63 %). In terms of water flux, the electrosprayed membrane exhibited lower value in filtrating HA solution compared to BSA solution and this could be due to higher rejection of membrane against HA which led to greater solutes accumulation on the membrane surface, increasing water transport resistance.

3.5. *Membrane stability test*

The stability of the membrane was studied by carrying out TGA, FT-IR and XPS tests. Fig. 7 demonstrates the TGA results of the electroprayed membrane before and after BSA and HA rejection. The TGA curves consisted of three main regions (30–172 °C, 172–500 °C and 500–600 °C), revealing different stage of membrane weight loss. The first region of the electrosprayed membrane weight loss was due to the loss of the remaining water in the membrane, while for PES-BSA and PES-HA membrane, the faster weight loss than the pristine

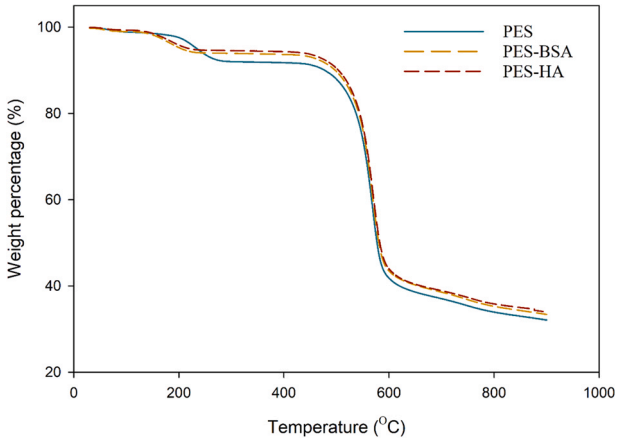

Fig. 7 – The TGA data of pristine PES membrane and PES membranes after BSA and HA filtration.

membrane was due to the presence of BSA and HA substances (on membrane) and water, respectively. The second weight loss was due to residual solvents (NMP and DMF) in all the membranes. The third weight loss was due to the cleavage of the C-O bond of PES polymer following polymer degradation at 500–600 °C.

When comparing the behaviour of the pristine PES membrane with thos of used membrane after 600 °C, it was found that the weight loss was almost similar. The greater residues on the used membranes can be attributed to the existence of HA and BSA on the top of the membrane and/or whithin the membrane pores. As a dead-end cell was used for the rejection test, the accumlation of the substances was expected.

Overall, this aspect of testing showed that the electrosprayed PES membrane had low tendency for fouling and this was concluded after conducting rejection tests using BSA and HA as model contaminants. Moreover, the TGA results confirmed that the electrosprayed PES membrane was thermally and mechanically more stable than the electrospun membranes reported elsewhere (Al-Ghafri et al., 2018; Al-Husaini et al., 2019a).

Further fouling investigation was carried out by FTIR analysis and the results are shown in Fig. 8. The existence of peaks at 3094 and 3062 cm^{-1} was corresponded to aromatic C-H stretch, while those at 1574 and 1481 cm^{-1} were attributed to aromatic C=C stretch. Peaks at 1296 and 1320 cm^{-1} were assigned to O=S=O bonding. These results clearly showed that there was no destruction of the functional groups of the polymer after rejection tests and that all the peaks have the same intensity, indicating that the electrosprayed PES membrane was not severly fouled by organic contaminants.

The surface properties of pristine PES membrane before and after filtration process were further analyzed using XPS and the results are shown in Fig. 9. The survey scans in Fig. 9a showed two main predominant peaks of C1s and O1s and other peaks of S2p and S2S for all membrane samples. Additional N1s peak was also detected for the membrane used for BSA filtration and this was probably due to the amine groups of BSA. Moreover, the silicon contaminant from DI water can be seen on the membranes used for HA and BSA filtration. High resolution C1s spectra of pristine PES and used membranes were further analysed with results

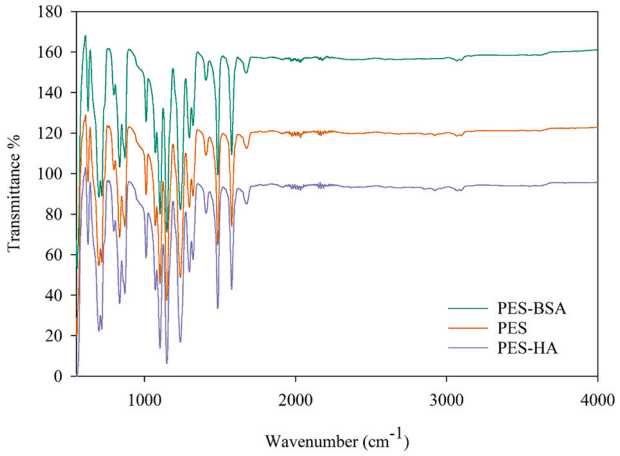

Fig. 8 – FTIR spectra of electrosprayed membrane before and after rejection test.

shown in in Fig. 9b-d. Four deconvoluted C1s features were obtained for the pristine membrane (Fig. 9b) at binding energy values of 283.8 eV (C═C), 284.6 eV (C-C/C-H), 286.3 eV (C-O) and 291.1 eV (π-π*) (Hong et al., 2018; Liu and Kim, 2011; Subtil et al., 2019). After subjecting the membrane to HA and BSA rejection (Fig. 9c-d), the deconvoluted high resolution C1s was obtained for five distinct peaks. They were C-C/C-H at 284.6 eV, the carbon atoms bonded to oxygen in hydroxyl components of HA and BSA (C-OH at 285.6 eV and C-OH at 285.4 eV), carbon atoms singly bonded to oxygen/nitrogen atoms (C-O at 286.3 eV and C-O/C-N at 286.2 eV), carbons in C═O at 288.6 eV from HA and carbons in O═C-O at 287.6 eV from BSA, and the shake-up satellite peak of π-π* at 291.6 eV (Ganguly et al., 2011; Jing et al., 2020; Miyake et al., 2016). Due to the accumulation of HA and BSA on the membrane surface, the reduction in C1s components of C-C/C-H and π-π* was observed (Table 3). Although HA and BSA were detected from the used membrane, the accumulated substances were not severe based on the water flux recovery results shown in Fig. 5 as well as TGA and FTIR analysis presented in Figs. 7 and 8, respectively.

Table 3 – C1s area (%) composition of pristine PES and used PES membrane.

Samples	Area (%) composition of C 1s						
	C═C	C-C/C-H	C-OH	C-O/ C-N	C═O	O═C-O	π-π*
PES	9.05	77.11	–	6.98	–	–	6.86
PES-HA	–	56.09	36.39	2.41	2.6	–	2.51
PES-BSA	–	48.99	36.49	6.86	–	5.39	2.26

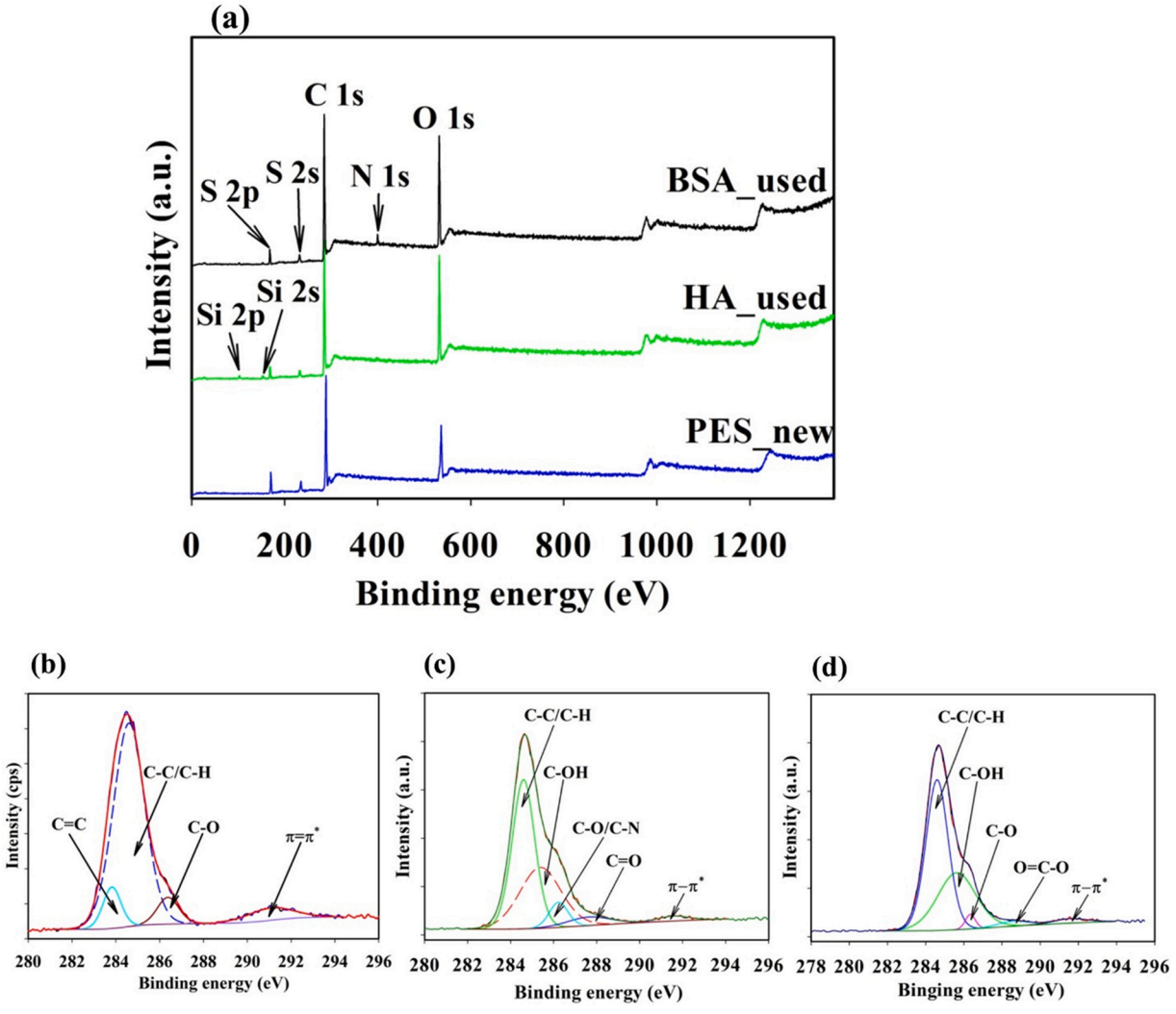

Fig. 9 – (a) XPS survey spectra and high resolution C1s spectra of (b) pristine PES, (c) HA-PES and (d) BSA-PES.

4. Conclusions

The results in this study showed that the new type of electrosprayed thin PES membrane has the potential to overcome the limitations of conventional membranes. The fabricated membrane has lower hydraulic resistance owing to its high porosity (~76 %) and can be operated at lower pressure. The electrospraying method is able to develop the membrane with several unique features compared to the electrospinning technique. As a comparison, the electrosprayed membrane has a smaller pore size (but similar porosity) and lower WCA. The new electrosprayed PES membrane also exhibit 35 % greater mechanical than that of an electrospun membrane. In terms of rejection, the electrosprayed membrane with thickness of 110 µm was able to achieve up to 81 % HA rejection and 63 % BSA rejection with water flux in the range of 80–88 $Lm^{-2}h^{-1}$ at 2 bar. Membrane fouling autopsy conducted using different instrument (FTIR, TGA and XPS) revealed that the electrosprayed membrane did not suffer from substantial fouling tendency. In conclusion, this study demonstrated an alternative way of designing and fabricating flat membrane using electrospraying technique that is potential to be used for macromolecules filtration.

Declaration of Competing Interest

The authors declare that they have no known competing financial interests or personal relationships that could have appeared to influence the work reported in this paper.

Acknowledgments

The authors would like to acknowledge Nanotechnology Research Center, Sultan Qaboos University, Oman for the technical support. The authors acknowledge His Majesty Trust Fund Strategic Grant (HMTF) for financial support under grant number SR/ENG/PCED/17/01. Moreover, the authors would like to thank Dr. Myo Tay Zar Myint from Surface Science Lab, Physics Department for conducting XPS test and Dr. Maissa Souayeh from Petroleum and Chemical Engineering Department for conducting viscosity measurements.

Appendix A. Supporting information

Supplementary data associated with this article can be found in the online version at doi:10.1016/j.cherd.2022.07.028.

References

Al-Ghafri, B., Bora, T., Sathe, P., Dobrestov, S., Al-Abri, M., 2018. Photocatalytic microbial removal and degradation of organic contaminants of water using PES fibers. Appl. Catal. B: Environ. 233, 136–142.

Al-Ghafri, B., Lau, W.-J., Al-Abri, M., Goh, P.-S., Ismail, A.F., 2019. Titanium dioxide-modified polyetherimide nanofiber membrane for water treatment. J. Water Process Eng. 32, 100970.

Al-Hinai, M.H., Sathe, P., Al-Abri, M.Z., Dobretsov, S., Al-Hinai, A.T., Dutta, J., 2017. Antimicrobial activity enhancement of poly (ether sulfone) membranes by in situ growth of ZnO nanorods. ACS Omega 2, 3157–3167.

Al-Husaini, I., Yusoff, A., Lau, W., Ismail, A., Al-Abri, M., Al-Ghafri, B., Wirzal, M., 2019a. Fabrication of polyethersulfone electrospun nanofibrous membranes incorporated with hydrous manganese dioxide for enhanced ultrafiltration of oily solution. Sep. Purif. Technol. 212, 205–214.

Al-Husaini, I.S., Yusoff, A.R.M., Lau, W.-J., Ismail, A.F., Al-Abri, M.Z., Wirzal, M.D.H., 2019b. Iron oxide nanoparticles incorporated polyethersulfone electrospun nanofibrous membranes for effective oil removal. Chem. Eng. Res. Des. 148, 142–154.

Bae, J., Baek, I., Choi, H., 2016. Mechanically enhanced PES electrospun nanofiber membranes (ENMs) for microfiltration: The effects of ENM properties on membrane performance. Water Res. 105, 406–412.

Baker, R.W., Staff, Ub, 2000. Membrane technology. Kirk-Othmer Encyclopedia of Chemical Technology.

Bhardwaj, N., Kundu, S.C., 2010. Electrospinning: a fascinating fiber fabrication technique. Biotechnol. Adv. 28, 325–347.

Bidlack, W.R., Tappel, A.L., 1973. Damage to microsomal membrane by lipid peroxidation. Lipids 8, 177–182.

Bonyadi, S., Chung, T.S., 2007. Flux enhancement in membrane distillation by fabrication of dual layer hydrophilic–hydrophobic hollow fiber membranes. J. Membr. Sci. 306, 134–146.

Buddanavar, A.T., Nandibewoor, S.T., 2017. Multi-spectroscopic characterization of bovine serum albumin upon interaction with atomoxetine. J. Pharm. Anal. 7, 148–155.

Chabalala, M.B., Al-Abri, M.Z., Mamba, B.B., Nxumalo, E.N., 2021. Mechanistic aspects for the enhanced adsorption of bromophenol blue and atrazine over cyclodextrin modified polyacrylonitrile nanofiber membranes. Chem. Eng. Res. Des. 169, 19–32.

Deitzel, J.M., Kleinmeyer, J., Harris, D., Tan, N.B., 2001. The effect of processing variables on the morphology of electrospun nanofibers and textiles. Polymer 42, 261–272.

Ganguly, A., Sharma, S., Papakonstantinou, P., Hamilton, J., 2011. Probing the thermal deoxygenation of graphene oxide using high-resolution in situ X-ray-based spectroscopies. J. Phys. Chem. C 115, 17009–17019.

Gopal, R., Kaur, S., Ma, Z., Chan, C., Ramakrishna, S., Matsuura, T., 2006. Electrospun nanofibrous filtration membrane. J. Membr. Sci. 281, 581–586.

He, M., Wang, Q., Wang, R., Xie, Y., Zhao, W., Zhao, C., 2017. Design of antibacterial poly (ether sulfone) membranes via covalently attaching hydrogel thin layers loaded with Ag nanoparticles. ACS Appl. Mater. Interfaces 9, 15962–15974.

Hernández, A., Calvo, J., Prádanos, P., Tejerina, F., 1996. Pore size distributions in microporous membranes. A critical analysis of the bubble point extended method. J. Membr. Sci. 112, 1–12.

Homaeigohar, S.S., Buhr, K., Ebert, K., 2010. Polyethersulfone electrospun nanofibrous composite membrane for liquid filtration. J. Membr. Sci. 365, 68–77.

Hong, G.-L., Zhao, H.-L., Deng, H.-H., Yang, H.-J., Peng, H.-P., Liu, Y.-H., Chen, W., 2018. Fabrication of ultra-small monolayer graphene quantum dots by pyrolysis of trisodium citrate for fluorescent cell imaging. Int. J. Nanomed. 13, 4807–4815.

Idris, A., Ismail, A., Noordin, M., Shilton, S., 2002. Optimization of cellulose acetate hollow fiber reverse osmosis membrane production using Taguchi method. J. Membr. Sci. 205, 223–237.

Jing, J., Zhang, S., Yuan, L., Li, Y., Lin, Z., Xiong, Q., Zhao, B., 2020. Combining humic acid with phosphate fertilizer affects humic acid structure and its stimulating efficacy on the growth and nutrient uptake of maize seedlings. Sci. Rep. 10, 17502.

Kassa, S.T., Hu, C.C., Keshebo, D.L., Ang, M.B.M., Lai, J.Y., Chu, J.P., 2020. Surface modification of high-rejection ultrafiltration membrane with antifouling capability using activated oxygen treatment and metallic glass deposition. Appl. Surf. Sci. 529, 147131.

Khin, M.M., Nair, A.S., Babu, V.J., Murugan, R., Ramakrishna, S., 2012. A review on nanomaterials for environmental remediation. Energy Environ. Sci. 5, 8075–8109.

Khulbe, K., Feng, C., Matsuura, T., Mosqueada-Jimenaez, D., Rafat, M., Kingston, D., Narbaitz, R., Khayet, M., 2007. Characterization of surface-modified hollow fiber polyethersulfone membranes prepared at different air gaps. J. Appl. Polym. Sci. 104, 710–721.

Lalia, B.S., Kochkodan, V., Hashaikeh, R., Hilal, N., 2013. A review on membrane fabrication: structure, properties and performance relationship. Desalination 326, 77–95.

Liu, S.X., Kim, J.-T., 2011. Characterization of surface modification of polyethersulfone membrane. J. Adhes. Sci. Technol. 25, 193–212.
Ma, D., Peng, B., Zhang, Y., Gao, B., Wang, Y., Yue, Q., Li, Q., 2014. Influences of dissolved organic matter characteristics on trihalomethanes formation during chlorine disinfection of membrane bioreactor effluents. Bioresour. Technol. 165, 81–87.
Miron, S.M., Dutournié, P., Thabet, K., Ponche, A., 2019. Filtration of protein-based solutions with ceramic ultrafiltration membrane. Study of selectivity, adsorption, and protein denaturation. Comptes Rendus Chim. 22, 198–205.
Missau, J., da Rocha, Jd.G., Dotto, G.L., Bertuol, D.A., Ceron, L.P., Tanabe, E.H., 2018. Purification of crude wax using a filter medium modified with a nanofiber coating. Chem. Eng. Res. Des. 136, 734–743.
Miyake, A., Komasa, S., Hashimoto, Y., Komasa, Y., Okazaki, J., 2016. Adsorption of saliva related protein on denture materials: an x-ray photoelectron spectroscopy and quartz crystal microbalance study. Adv. Mater. Sci. Eng. 2016, 5478326.
Mo, H., Tay, K.G., Ng, H.Y., 2008. Fouling of reverse osmosis membrane by protein (BSA): effects of pH, calcium, magnesium, ionic strength and temperature. J. Membr. Sci. 315, 28–35.
Moradi, G., Zinadini, S., Rajabi, L., 2020. Development of nanofiltration PES membranes incorporated with hydrophilic para hydroxybenzoate alumoxane filler for high flux and antifouling property. Chem. Eng. Res. Des. 158, 148–163.
Rojas, S., Horcajada, P., 2020. Metal–organic frameworks for the removal of emerging organic contaminants in water. Chem. Rev. 120, 8378–8415.
Selatile, M.K., Ray, S.S., Ojijo, V., Sadiku, R., 2018. Recent developments in polymeric electrospun nanofibrous membranes for seawater desalination. RSC Adv. 8, 37915–37938.
Shaulsky, E., Nejati, S., Boo, C., Perreault, F., Osuji, C.O., Elimelech, M., 2017. Post-fabrication modification of electrospun nanofiber mats with polymer coating for membrane distillation applications. J. Membr. Sci. 530, 158–165.
Subtil, E., Gonçalves, J., Gajardoni de Lemos, H., Venancio, E., Mierzwa, J., Souza, J., Alves, W., Le-Clech, P., 2019. Development of a new composite conductive porous membrane (PES/PANI/RGO) for electrochemical fouling mitigation.
Sweet, M.L., Pestov, D., Tepper, G.C., McLeskey Jr., J.T., 2014. Electrospray aerosol deposition of water soluble polymer thin films. Appl. Surf. Sci. 289, 150–154.
Takeshi, K., Takagi, K., Fukuda, T., Chihara, T., Tajima, Y., 2013. Film-forming properties of fullerene derivatives in electrospray deposition method. J. Surf. Eng. Mater. Adv. Technol. 3, 84.
Tański, T., Matysiak, W., Krzemiński, Ł., Jarka, P., Gołombek, K., 2017. Optical properties of thin fibrous PVP/SiO2 composite mats prepared via the sol-gel and electrospinning methods. Appl. Surf. Sci. 424, 184–189.
Tsai, C.-Y., Tam, S.-Y., Lu, Y., Brinker, C.J., 2000. Dual-layer asymmetric microporous silica membranes. J. Membr. Sci. 169, 255–268.
Uzal, N., Ates, N., Saki, S., Bulbul, Y.E., Chen, Y., 2017. Enhanced hydrophilicity and mechanical robustness of polysulfone nanofiber membranes by addition of polyethyleneimine and Al2O3 nanoparticles. Sep. Purif. Technol. 187, 118–126.
Vatanpour, V., Rabiee, H., Farahani, M.H.D.A., Masteri-Farahani, M., Niakan, M., 2020. Preparation and characterization of novel nanoporous SBA-16-COOH embedded polysulfone ultrafiltration membrane for protein separation. Chem. Eng. Res. Des. 156, 240–250.
Wang, F., Zheng, T., Xiong, R., Wang, P., Ma, J., 2019. CDs@ ZIF-8 modified thin film polyamide nanocomposite membrane for simultaneous enhancement of chlorine-resistance and disinfection byproducts removal in drinking water. ACS Appl. Mater. Interfaces 11, 33033–33042.
Wang, J., Cao, B., Zhang, R., Li, P., 2022. Spray-coated tough thin film composite membrane for pervaporation desalination. Chem. Eng. Res. Des. 179, 493–501.
Wang, Z., Crandall, C., Sahadevan, R., Menkhaus, T.J., Fong, H., 2017. Microfiltration performance of electrospun nanofiber membranes with varied fiber diameters and different membrane porosities and thicknesses. Polymer 114, 64–72.
Yang, Q., Wang, K.Y., Chung, T.-S., 2009. A novel dual-layer forward osmosis membrane for protein enrichment and concentration. Sep. Purif. Technol. 69, 269–274.
Zhao, X., Chen, Y., Xuan, H., He, C., 2016. Investigation of one-dimensional multi-functional zwitterionic Ag nanowires as a novel modifier for PVDF ultrafiltration membranes. N. J. Chem. 40, 441–446.
Zhu, S., Shi, M., Zhao, S., Wang, Z., Wang, J., Wang, S., 2015. Preparation and characterization of a polyethersulfone/polyaniline nanocomposite membrane for ultrafiltration and as a substrate for a gas separation membrane. RSC Adv. 5, 27211–27223.